PART I

Structures, Properties, and Design Rules in Hierarchical Materials in Nature

CHARACTERIZATION OF THE COMPLEX MATRIX OF THE *MYTILUS EDULIS* SHELL AND THE IMPLICATIONS FOR BIOMIMETIC CERAMICS

J.A. Keith*, S.A. Stockwell*, D.H. Ball*, W.S. Muller*, D.L. Kaplan*, T.W. Thannhauser**, R.W. Sherwood**
*Biotechnology Division, US Army Natick RD&E Center, Natick, MA 01760-5020 USA
**Analytical and Synthesis Facility, Cornell University Biotechnolgy Core Facility, Ithaca, NY 14853

ABSTRACT

The macromolecular matrix present in the composite shell of the blue mussel, *Mytilus edulis,* accounts for less than 1% of the shell by weight but is theorized to play a significant role in controlling the growth, morphology, and orientation of the $CaCO_3$ that makes up the shell. The presence of several proteins in this matrix, only some of which have affinity for calcium, suggests a hierarchical structural model for the shell. Proteins were isolated under denaturing, reducing conditions and separated by centrifugation, gel electrophoresis, and high performance liquid chromatography. The major matrix proteins, both soluble and insoluble, were evaluated for amino acid composition, calcium binding, and glycosylation. Some N-terminal sequence data was collected. Non-proteinaceous components of the matrix were also analyzed. Comparison of the mussel shell matrix with the protein matrix of other molluscan systems suggests that this complexity is not unique to the mussel and may provide a key to the understanding of more generic biomineralization processes necessary for such applications as biomimetic ceramics.

INTRODUCTION

The formation of molluscan shell structures or composites containing calcium carbonate involves control over crystal morphology, size, density, and orientation at the molecular level that is at present unattainable synthetically. The organic portion of most mollusc shells, consisting of 0.1 to 5 % by weight of the total structure [1], is postulated to be the source of this control [2-5].

A review of the literature shows a variety of compositions and functionalities assigned to this organic portion, termed the matrix, including proteins; specifically proteoglycans [6], phenyloxidase crosslinked proteins[7], and phosphoproteins [8-10], as well as polysaccharides such as chitin [11, 12], sulfated mucopolysaccharides [13, 14], neutral and amino sugars [1,15], and lipids [16] . Characterization of the matrix composition varies with species of mollusc [1, 3, 17, 18] and methodology [19]. Past attempts to characterize this organic matrix have focused on a soluble proteinaceous fraction with acidic functionality which inhibits crystallization [18, 21,22], isolated mainly from *Mercenaria mercenaria, Crassostrea virginica,* or *Mytilus californianus* [3, 15, 20]. To begin to determine the mechanisms involved in the biomineralization process, a complete analysis of the organic matrix of *Mytilus edulis* was performed. This species of mollusc was in part chosen for the complexity of the shell, which consists of an inner nacreous layer of aragonite, a pallial calcitic layer, and an outer prismatic layer of calcite [23-25]. It was believed that this level of structural complexity would lead to a better understanding of the complexity of control attributed to these organic matrices.

The objective of this work was to analyze the organic components and purified individual proteins from the matrix for amino acid content using microanalytical methods and to begin to understand relationships between protein structure and mineral binding function. Analysis of the protein, polysaccharide, and lipid portions of this organic matrix has revealed many components, including several proteins of discrete molecular weight, amino acid composition and glycosylation pattern.

Mat. Res. Soc. Symp. Proc. Vol. 255. ©1992 Materials Research Society

EXPERIMENTAL

Live specimens of *Mytilus edulis* were collected locally (Marshfield, MA), maintained in seawater and processed within 24 hours of collection. Soft tissue was removed, the shells were scrubbed with 5% NaOH to remove the periostracum and any adhering organisms and then lightly crushed with a mortar and pestle. The crushed shell was ground to a fine powder in a freezer mill under liquid nitrogen and stored at -70°C. Obtained from The Abalone Farm (Cuyurcus,CA), *Haliotis rufescens* shells were processed in the above manner within 24 hours of soft tissue removal. Extraction of macromolecules was carried out over 3 days by stirring 40 g of powdered shell at 4°C in 2 liters of guanidine/EDTA buffer modified from Butler [26]. The protease inhibitor aprotinin (3mg/liter) replaced the soybean trypsin inhibitor and pepstatin in Butler's extraction and the EDTA concentration was reduced from 0.5M to 0.25M. Two liters of solution can be used to process 40 g of powdered shell in 2-3 days. The extract was centrifuged at 10,000 rpm for 20 minutes to separate the "soluble matrix" (supernatant) from the insoluble matrix (pellet), with a final yield of about 40 mg from 40 g of shell. Preparations were then dialyzed exhaustively against Milli-Q™ water and lyophilized.

Protein content of the purified soluble matrix material was determined by Lowry assay with a deoxycholate trichloroacetic acid precipitation [27]. Protein content of purified insoluble matrix material was determined by elemental carbon, hydrogen, and nitrogen analysis performed by Oneida Research Services (Whitesboro, NY). Polyacrylamide gel electrophoresis and Western blotting to PVDF membranes were performed on a Novex™ Gel Electrophoresis system (Novel Experimental Technology, Encinitas, CA), with Novex™ Tris-Gly and Tricine buffers and gradient gels.

Amino acid analysis of the purified matrix as well as protein bands purified by PAGE was performed by derivatization after hydrolysis, and reverse phase HPLC using the Waters Pico-Tag™ method (Waters, Division of Millipore, Milford, MA). Analysis of lower molecular weight individual protein bands transfered to PVDF membranes was that of LeGendre and Matsudaira [28], while the standard manufacter's protocols [29] were used for the total soluble and insoluble matrix proteins. Controls consisting of a section of membrane without protein were run with each sample to correct for backround.

Glycosylation of purified proteins and carbohydrate content of the matrix after hydrolysis were determined by the method of Chaplin [30] which utilizes methanolysis to convert polysaccharides to their methyl glucosides, followed by dervatization to trimethylsiloethers. Gas liquid chromatographic (GLC) analysis of these derivatives was done with a Hewlett Packard (Andover, MA) gas chromatograph, Model 5880A, equipped with a flame-ionization detector and a J&W Scientific (Rancho Cordova, CA) fused silica capillary column, 30m x 0.26mm i.d.: liquid phase DB1 (equivalent to SE 30), film thickness 0.1 µm. Detection limit is 100 picomoles.

Calcium binding was assayed using a modification of a procedure from Maruyama et al. [31]. Proteins purified from the matrix were solubilized and blotted onto nitrocellulose and dried at room temperature. The nitrocellulose was washed for 1 hour in 60 mM KCl, 5 mM $MgCl_2$ and 10 mM imidazole-HCl (pH 6.8). The membrane was washed for 15 minutes in the same buffer containing 5 mM $^{45}Ca^{2+}$ and rinsed with 50% EtOH. After drying, the membrane was placed in a film cassette with X-ray film and exposed for 24 to 48 hours before developing. Phosvitin (Sigma Chemical Co, St Louis, MO), an eggshell protein, was used as a positive control and aprotinin (Sigma Chemical Co, St. Louis, MO), a protease inhibitor, as the negative control. Autoradiographs were scanned with an UltraScan™XL laser densitomer (Pharmacia LKB Biotechnology, Uppsala, Sweden).

RESULTS AND DISCUSSION

Total soluble protein content of the shell is 0.3-0.5% by weight when determined by Lowry assay. Although the values from the Lowry assays were used in subsequent purification steps, visual inspection of gel staining suggested that the Lowry determination of soluble protein content may be low. This can be accounted for by the fact some proteins have a differential response to the assay [27]. The precipitation step allows the Lowry assay to be used in the presence of EDTA and other interfering substances [27] , but can reduce recovery by half (Sigma procedure #P 5656).

Insoluble material, determined to be 91-100% protein by elemental analysis (Table I), accounts

for 2-5% of the shell by weight; together the soluble and insoluble proteins make up about 3-5% of the shell. No glucosamine or N-acetyl glucosamine derivatives, which would indicate the presence of chitin or chitosan, were found during GLC analysis of the insoluble material and of powdered shell, further supporting the elemental analysis determination that the matrix is composed almost completely of protein. This contradicts the common assertion that chitin is omnipresent in molluscan organic matrixes [4] . The amino acid composition of the insoluble matrix indicates a predominance of Gly, Ala, and Ser residues (65%), which is characteristic of silk structures and comparison of the amino acid composition of the insoluble matrix to spider dragline silk [32] indicates strong similarities (Table II). A beta-sheet structure has been suggested as a key scaffolding element in the organic matrix of the shell based on X-ray diffraction analysis [20,33], and the composition of the mussel shell insoluble matrix reported here is consistent with this hypothesis.

Table I. Elemental Analysis of Insoluble Matrix. Total protein is calculated by using an average value of 6.25% nitrogen for protein, which can vary with amino acid content, explaining why total protein is greater than unity.

Sample #	% carbon	%hydrogen	%nitrogen
1	41.64	5.65	17.23
2	41.44	5.59	17.24
Total protein (average)[1]	high 107%	low 91%	

[1] Based on conversion of nitrogen x 6.25% for high value, 5.30% for low [34]. These values cover most proteins, including structural proteins like silk and collagen.

Table II. Comparison of amino acid compositions of matrix with other proteins. Figures given are mole %, not adjusting for Trp, which cannot be detected by Pico-Tag™ analysis.
* from *Nephila clavipes* [32] ** from *Strongylocentrtus purpuratus* [35].

amino acid	Insoluble matrix	Spider dragline silk*	Sea Urchin spicule matrix**	Soluble matrix
Gly	27.8	37.1	21.3	20.5
Ala	26.1	21.1	8.3	11.6
Ser	10.9	4.5	12.5	9.3
Asx	10.6	2.5	11.0	13.0
Leu	4.9	3.8	4.2	5.2
Glx	3.5	9.2	12.1	7.5
Arg	2.6	7.6	2.3	4.4
Lys	2.5	<1.0	3.3	5.2
Val	2.3	1.8	3.4	4.2
Phe	2.0	-	1.8	2.9
Tyr	1.9	2.9	1.3	2.5
Ile	1.6	<1.0	2.5	5.2
Thr	1.3	1.7	4.4	2.8
Pro	1.0	4.3	4.5	3.4
Met	<1.0	<1.0	<1.0	1.1
His	<1.0	-	3.7	3.2
Cys	<1.0	<1.0	2.9	<1.0

The soluble protein portion of the matrix has four major protein components and several minor protein components. The four major protein components were identified by SDS PAGE; in the absence of reducing agents, they run at about 200 kDa, 95 kDa, 32 kDa and 21 kDa. Adding 2-mercaptoethanol to the sample buffer eliminates the 200 kDa band, greatly intensifies the 95 kDa band, and eliminates shadow bands on either side of the 21 kDa band. The elimination of the 200 kDa band and intensification of the 95 kDa band upon addition of 2-mercaptoethanol to the

sample buffer suggests that the larger protein consists of two subunits of the smaller. The elimination of the shadow bands on either side of the 21 kDa band by reducing agent also suggests that these two bands are conformational isomers of the major band at 21 kDa.

Table III. Amino acid composition of individual proteins from the mussel soluble matrix and comparison with sea urchin matrix. Figures given are mole %, not adjusting for Trp, which cannot be detected by Pico-Tag™ analysis. *Indicates amino acids most sensitive to PVDF membrane procedure.**Amino acid not detected by Pico-Tag™ analysis. Sea urchin figures are from the actual gene sequence [41].

amino acid	95kDa	32 kDa	21 kDa	50 kDa protein from sea urchin
Gly	1.0	17.7	24.2	8.0
Glx	18.8	13.3	6.1	12.9
Ser	6.0	12.1	9.9	5.4
Asx	18.5	9.5	8.2	15.4
Ala	11.9	6.2	8.6	8.9
Leu	8.9	5.4	7.7	2.9
Arg	7.0	4.9	3.9	4.7
Val	4.3	4.8	4.3	11.4
Lys	5.3	4.7	4.1	1.1
Pro	3.4	4.5	5.0	7.4
Thr	3.9	4.4	4.3	4.5
Ile	3.8	3.1	3.8	3.6
Phe	1.3	2.7	4.0	2.5
His	1.3	2.3	1.1	<1.0
Tyr*	2.2	2.0	3.5	1.6
Met*	3.1	1.6	<1.0	2.5
Cys*	<1.0	<1.0	<1.0	1.4
Trp**	-	-	-	6.3

Amino acid analysis of the soluble proteins is reported in Table 3. The lower molecular weight proteins have similar compositions with an abundance of Gly, Glx and Ser residues. The composition of the total soluble matrix (Table II) is over 40% small amino acids (Gly, Ala, Ser), with another 20% comprised of Asx and Glx. The amino acid composition of the 95 kDa protein is significantly different from the 32 and 21 kDa proteins, containing 46% Asx and Glx residues. Of the four primary soluble bands purified, only the 95 kDa protein is glycosylated, containing N-acetyl glucosamine, and alpha and beta glucose, in a ratio of 1:3:4. The composition of the total soluble matrix (Table III) bears some similarity to the spicule matrix from *Strongylocentrus purpuratus* [35], especially in the percentages of Gly, Ala, Ser, Asx, and Glx, which make up 60% of the two matrix fractions. The amino acid composition of the 95 kDa protein suggests that it may be the acidic fraction often referred to in the literature as having an influence on crystallization [21, 36, 37]. Some researchers report difficulty in staining these types of acidic proteins [38] , however when poor staining was observed in the current study it was often attributable to insufficient protein concentration. Butler et al. [39], was able to stain acidic rat glycoproteins with Coomassie blue and Weiner et al. [40], had earlier reported staining of *Mytilus* proteins with Coomassie blue. Comparison of the 95 kDa protein with the 50 kDa protein from sea urchin spicules sequenced by Sucov et al. [41] (Table III) shows similar amounts of Glx, Asx and Ala; the only significant differences between them are the percentage of Val and Gly residues.

Preliminary results indicate both total soluble matrix and total insoluble matrix bind calcium under the assay conditions studied, in a weight ratio equal to phosvitin. To confirm that the calcium binding observed was not an artifact created by residual EDTA in the matrix preparations, a problem noted by others [42, 43], both EDTA and GLC analysis were used as controls. GLC was able to detect an EDTA adduct when EDTA remained in matrix preparations, and the protein components which bound calcium were shown to be free of EDTA by this method. Since both matrices bind calcium under the assay conditions studied, this suggests that calcium binding is not limited to anionic proteins, and may involve an ionotropy, a change in affinity for calcium resulting from already bound calcium carbonate, as suggested by Sikes and Wheeler [8]. It should be noted that the assay used characterizes calcium affinity of proteins immobilized on membranes, which may be different from calcium affinity of protein free in solution [5] and does not incorporate any interactions with other macromolecules which may be present *in vivo*. This immobilization assay may still be more representative of *in vivo* conditions than free solution measurements if it is immobilized protein which initiates crystallization, as suggested by Linde et al. [44]. Aside from differences in soluble versus insoluble conditions for the assay, subtle changes in protein conformation under the assay conditions could also impact on calcium binding affinity.

The findings that both the acidic soluble matrix proteins and the more neutral insoluble matrix proteins bind calcium, despite differences in amino acid composition and functionality, and that chitin is not present in the *Mytilis edulis* matrix, indicate that the *in vivo* conditions may be more complex than suggested by models of matrix-mediated crystallization which assign calcium interaction to the acidic macromolecules and structural support to a chitin-based polysaccharide coupled to a silk-like protein component [6,45]. Further research on the structural, temporal and molecular recognition issues associated with the matrix macromolecules may reveal that more complex interactions, such as between several organic components, may be required to mediate controlled crystal growth in molluscan shells. This level of understanding may be required before biomimetic approaches to this process can be fully realized.

ACKNOWLEDGEMENTS

Naomi Darling for protein preparations, and Hap Wheeler, Richard Laursen and Stephen Weiner for helpful discussions.

REFERENCES

1. P.E. Hare and P.H. Abelson, Carnegie Institution Yearbook, 64, 223 (1965).
2. K. Wilbur, in Physiology of Mollusca, Vol I, edited by K.M. Wilbur and C.M. Yonge, (Academic Press, New York, NY. 1964), p. 243.
3. G. Krampitz, J. Engels, and C. Cazaux, in The Mechanisms of Mineralization in Invertebrates and Plants, edited by N. Watabe, and K.M. Wilbur, (University of South Carolina Press 1976), p. 155.
4. H.A. Lowenstam and S. Weiner, On Biomineralization, (Oxford University Press, New York, NY, 1989).
5. A.P. Wheeler and C.S. Sikes, in Biomineralization Chemical and Biochemical Perspectives, edited by S. Mann, J. Webb, and R.P. Williams, (VCH Publishers, New York, NY. 1989) p. 95.
6. S. Weiner, W. Traub, and H.A. Lowenstam, in Biomineralization and Biological Metal Accumulation, edited by P. Westbroek and E.W. deJong, (D. Reidel Publishing Co., Dordrecht, Holland, 1983) p. 205.
7. J. Gordon and M.R. Carriker, Mar. Biol., 57, 251, (1980).
8. C.S. Sikes and A.P. Wheeler, in Biomineralization and Biological Metal Accumulation, edited by P. Westbroek and E.W. DeJong, (D. Reidel, Dordrecht, Holland 1983), p. 285.
9. D.M. Swift, C.S. Sikes, and A.P. Wheeler, J. Exp. Zool., 240, 65 (1986).
10. D.J. Veis, T.M. Albinder, J. Clohisy, M. Rahima, B. Sabsay, and A. Veis, J. Exp. Zool., 240, 35 (1986).
11. C. Jeuniaux, Chitine et Chitinolyse, (Masson, Paris, France 1963)
12. W. Peters, Comp. Biochem. Biophysiol, 41B, 541 (1972).

13. K. Simkiss, Comp. Biochem. Physiol., 16, 427 (1965).
14. M.A. Crenshaw, and H. Ristedt, in The Mechanisms of Mineralization in the Invertebrates and Plants, edited by N. Watabe and K.M. Wilbur, (University of South Carolina Press, 1976), p. 355.
15. M.A. Crenshaw, Biomineralization, 6, 6, (1972).
16. G.E. Beedham, Quart. J. Microsc. Sci., 99, 341, (1958).
17. V.R. Meenakshi, P.E. Hare, and K.M. Wilbur, Comp. Biochem. Physiol., 40B, 1037 (1971).
18. S. Weiner and L. Hood, Science, 190, 987 (1975).
19. G. Krampitz, H. Drolshagen, and S. Hotta, Experientia, 39, 1104 (1983).
20. S. Weiner and W. Traub, in Structural Aspects of Recognition and Assembly in Biological Macromolecules, edited by M. Balaban,J.L. Sussman, W. Traub, and A. Yonath, (Balaban ISS 1981), p. 467.
21. S. Weiner, in The Chemistry and Biology of Mineralized Connective Tissues, edited by A. Veis, (Elsevier North Holland, Inc. 1981), p. 517.
22. C.S. Sikes and A.P. Wheeler, Chemtech, Oct., 620 (1988).
23. C. Gregoire, J. Biophys. Biochem. Cytol., 9, 395, (1961); in Chemical Zoology, Vol 7, edited by M. Florkin and B.T. Scheer, (Academic Press, New York, 1972), p. 45.
24. W.J. Kennedy, J.D. Taylor, and A. Hall, Biol. Rev., 44, 499 (1969).
25. M.R. Carriker, Mar. Biol., 48, 105, (1978).
26. W.T. Butler, in Methods in Enzymology, Vol 145, edited by L.W. Cunningham, (Academic Press, New York, 1987), p. 290.
27. G.L. Peterson, Anal. Biochem., 83, 346 (1977).
28. N. LeGendre and P. Matsudaira, Biotechniques, 6 (2), 154 (1988).
29. S.A. Cohen, M. Meys,and T.L. Tarvin, T.L., The Pico-Tag™ method, A manual of advanced techniques for amino acid analysis, (Waters Division of Millipore, Milford, MA USA, 1989).
30. M.F. Chaplin, Anal. Biochem, 123, 336, (1982).
31. K. Maruyama, T. Mikawa, and S. Ebashi, J. Biochem, 95, 511 (1984).
32. S. Lombardi and D. Kaplan, J. Arachnol., 18, 297 (1990).
33. S. Weiner and W. Traub, FEBS Letters, 111 (2), 311 (1980).
34. Agricultural Research Service, Composition of Foods, Handbook 8, (USDA, Washington, DC, USA, 1963).
35. S.C. Benson, N.C. Benson, and F. Wilt, J. Cell Biol., 102, 1878, (1986).
36. L. Addadi and S. Weiner, Proc. Natl. Acad. Sci. USA, 82, 4110 (1985); Mol. Cryst. Liq. Crystal, 13, 305 (1986).
37. A. Berman, L. Addadi, and S. Weiner, Nature, 331, 546 (1988).
38. S. Weiner, J. Chrom., 245, 148 (1982).
39. W.T. Butler, M. Bhown, M.T. Dimuzio, and A. Linde, Coll. Res., 1, 187, (1981) .
40. S. Weiner, H.A. Lowenstam, and L. Hood, J. Exp. Mar. Biol. Ecol., 30, 45 (1977).
41. H.M. Sucov, S. Benson, J.J. Robinson, R.J. Britten, F. Wilt, and E.H. Davidson, Dev. Biol., 120, 507 (1987).
42. S. Weiner, Calcif. Tissue Int., 29, 163 (1979).
43. A.P. Wheeler, K.W. Rusenko, J.W. George, and C.S. Sikes, Com. Biochem. Physiol., 87B (4), 953 (1987).
44. A. Linde, A. Lussi, and M.A. Crenshaw, Calcif. Tissue Int., 44, 286 (1989).
45. S. Weiner and W. Traub, Phil. Trans. R. Soc. London Ser. B, 304, 421 (1984) .

A HIERARCHICALLY STRUCTURED MODEL COMPOSITE: A TEM STUDY OF THE HARD TISSUE OF RED ABALONE

JUN LIU, MEHMET SARIKAYA, and ILHAN A. AKSAY
Department of Materials Science and Engineering, and
Advanced Materials Technology Center, Washington Technology Center,
University of Washington, Seattle, WA 98195

ABSTRACT

The structure and crystallography of the nacre of red abalone, Haliotis rufescens, *was studied by transmission electron microscopy imaging and diffraction. We found that the nacre structure is based upon hierarchical {110} twinning in aragonite with the following organization: (i) first generation twins between platelets having incoherent boundaries, (ii) second generation twins between domains having coherent boundaries within a given platelet, and (iii) nanometer-scale third generation twins within domains. Since the aragonite platelets nucleate and grow as separate crystals, this long-range crystallographic relationship between the inorganic units of a biological hard tissue indicates that the nucleation and growth process of crystals may be mediated by the organic matrix and that the organic template structure may also be long-range ordered. We propose a superlattice structure based on the possible twin variants and suggest that the organic matrix structure, or the arrangement of nucleation sites, is compatible with the superlattice. Multiple tiling based upon this superlattice allows all of the crystallographic and morphological platelet configurations observed in nacre.*

INTRODUCTION

Nacre is a laminated ceramic-polymer composite material found in mollusk shells.[1-6] It has a highly ordered structure on a continuous scale[1] from the nanometer to the millimeter and has unique mechanical properties, such as high fracture toughness and strength.[3-4] Understanding its structure, in particular the growth process and the interrelationships between the microstructure and properties, is valuable to biological sciences, materials science and engineering, and the electronic industry. Previous studies have suggested that the formation of the inorganic crystals was regulated by the organic matrix through epitaxial growth.[6-9] But to date neither the structure of the inorganic phase with its detailed architecture nor the organic phase have been fully understood. In nacre, the inorganic phase, $CaCO_3$ in the aragonite form (Pmcn, No. 62), and the organic phase, a mixture of proteins and polysaccharides,[8-9] are arranged in a "brick and mortar" microarchitecture (Figure 1).[1-5] The aragonite platelets, with hexagonal or square faces, are about 5 μm in edge length and 0.25 to 0.5 μm in thickness, and the organic phase is about 100-200 Å thick.[10] Previous diffraction studies[11] illustrated that the platelets on a given layer are aligned in the *c* direction of the orthorhombic unit cell of the aragonite lattice. It was further suggested that the platelets are arranged in a "mosaic pattern" without definite crystallographic relationships between them in the *a-b* plane.[12] Similarly, it was suggested that only local ordering existed in the organic matrix, which was thought to be responsible for the mosaic polycrystalline pattern in the aragonite crystals.[12]

Mat. Res. Soc. Symp. Proc. Vol. 255. ©1992 Materials Research Society

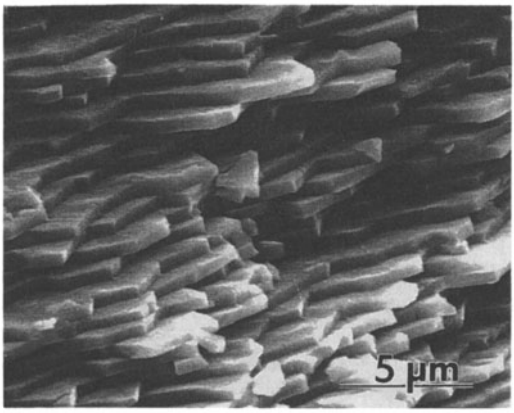

Figure 1. Secondary electron image of fractured surface of nacre reveals the brick and mortar microarchitecture. Nacre is from a pearl oyster sample (*Pinctada margaritifera*). Courtesy of Katie E. Gunnison.

Contrary to these earlier studies, in the following sections, we summarize our recent electron microscopic studies to show that platelets have definite crystallograhic relationships to each other and are arranged with levels of hierarchical twins. Our findings also suggest the existence of a long-range order in the organic matrix.

CRYSTALLOGRAPHY OF ARAGONITE PLATELETS: HIERARCHICAL TILING IN THE NACRE STRUCTURE

We first studied both the geometrical arrangement of and the crystallographic relationship among the aragonite platelets.[1,13] In the face-on view, each layer of the nacre is composed of closely packed platelets (Figures 2(a) and 2(b)). The platelets have either three, four, five, or six edges. The geometrical organization of the platelets often exhibits sixfold symmetry as shown in Figures 2(a) and 2(b) where six platelets are arranged with an approximate 60° angle between each pair (60° twin boundaries). The crystallographic orientations between the platelets on the *a-b* plane are not random, contrary to previous assumptions,[11-12] but generally relate to one another by twinning, as shown by the diffraction patterns in Figures 2(c) and 2(d). The [001] single crystalline pattern in Figure 2(c) is from the interior of a platelet; the pattern in Figure 2(d), which was recorded from the boundary between two platelets, incorporates two superimposed patterns. Analysis of the two patterns reveals that they are correlated to each other by a twin relationship, with the twin plane {110} parallel to the [001] direction of the crystal, i.e., either (110) or $(1\bar{1}0)$. The images in Figures 2(a) and 2(b) were recorded by tilting the